VTL-PUB-45
(SEPTEMBER 1977)

NEUTRINO RESULTS FROM THE FERMILAB 15-FOOT BUBBLE CHAMBER USING NEON-HYDROGEN MIXTURES*

T. H. Burnett

Visual Techniques Laboratory, Department of Physics
University of Washington, Seattle, Washington 98195

ABSTRACT

Neutrino results from the FNAL 15-boot bubble chamber, using two different neon-hydrogen mixtures are reviewed. Included are the measurements from four different experiments of the dilepton, or μe rate, which appear to be consistent with the charm production interpretation for this process. Also mentioned is a study of the scaling variable distributions for anti-neutrinos, which shows no anomalous threshold, consistent with the usual four-quark model, but indicates a slight scale breaking. The ratio of $\bar{\nu}n$ to $\bar{\nu}p$ cross sections has been extracted from the same data and is also consistent with the quark model. A study of the hadronic state produced by electron (anti)neutrinos in neon is summarized, with the conclusion that nuclear rescattering effects are the same as for hadron interactions.

*Invited talk presented to the 1977 International Symposium on Lepton and Photon Interactions at High Energies

FERMILAB-CONF-77-152-E

E172

I. INTRODUCTION

This review covers (anti)neutrino charged current (CC) results obtained by four experiments using the Fermilab 15' bubble chamber filled with mixtures of neon and hydrogen. The chamber is basically a sphere 4 m in diameter, giving a usable volume of $\sim 25\ m^3$, or a target mass of 20 tons or 8 tons for the two mixtures which have been used. All experiments had available to them data from the external muon identifier (EMI), $24\ m^3$ of proportional chambers behind 3-5 interaction lengths of copper from the magnet coils, or zinc placed as an absorber. Note that with a punch-through probability of $\sim 5\%$ and a comparable probability for correlation of an extrapolated leaving track with an uncorrelated background signal, the EMI can perform hadron-muon separation only in a statistical sense.

A summary of the experiments, with respective running conditions and exposures reported on to date, is given in Table I. The four experiments are classified according to whether they used the "light" (21% Ne atomic) or "heavy" (64% Ne atomic) mixture and whether the broad-band-horn-focused beam was set for neutrinos or antineutrinos. Note that the beams were rather different for the two antineutrino experiments - BHS used only one horn without a plug to obtain nearly equal numbers of neutrino and antineutrino events, while FIIM had both horns and an absorptive plug to achieve a neutrino contamination of less than 4%. Advantages of the former are the ability to make ν-$\bar{\nu}$ comparisons and the latter, the pure beam necessary for neutral current studies.

The heavy mixture has several advantages over the light: the higher density (0.8 v. 0.3 gcm^{-3}) results in a correspondingly higher event rate; the shorter radiation length (40 cm v. 1.3 m) allows much easier electron identification, of importance for the μe searches discussed below; the shorter interaction length (1.3 v. 3 m) reduces the number of hadrons that leave the chamber without interacting, making hadron-muon separation easier; and finally the shorter radiation and interaction lengths in conjunction allow detection of much of the neutral energy. Disadvantages are that interactions and pair conversions close to the primary vertex make measurements difficult or impossible, a problem that becomes more serious with increasing energy; showers can obscure important details, as K^o or Λ decays; and the momenta of energetic electrons is often difficult to measure.

In the following, the data will frequently be compared with the quark model, specifically the 4-quark model with charm. Except for the strange sea, the quark momentum distributions of Field and Feynman (FF)[1] have been used. Since these distributions are based primarily on electron scattering, which leaves the strange quark contribution essentially undetermined, I have used the CDHS dimuon antineutrino results.[2] These, interpreted as charm production from the strange sea, indicate that $0.05\ (1-x)^7$ better represents the data than the FF guess of $0.1\ (1-x)^8$. It should also be noted that the u- and d-antiquark distributions are only poorly determined from electroproduction data, so discrepancies with antineutrino distributions, which are sensitive to antiquarks, should be considered as pointing the way to a better determination of these functions.

TABLE I

Summary of the neon-hydrogen mixtures and wide band beams used by the experiments reported on.

Ne-H Mixture	light 21% Ne at.		heavy 64% Ne at.	
Density	0.3 g cm^{-3}		0.8 g cm^{-3}	
Radiation length	1.4 m		0.4 m	
Interaction length	3 m		1.3 m	
Institutions	WBHC Wisconsin LBL Hawaii CERN	FIIM FNAL IHEP ITEP Michigan	CB Columbia BNL	BHS Berkeley Hawaii Seattle
Beam	300 GeV protons ν 2 horns	300 GeV $\bar{\nu}$ 2 horns plug	400 GeV ν 2 horns	400 GeV $\bar{\nu}$ 1 horn
Pictures (subsequent run)	70K -	75K (180K)	46K (100K)	49K -
CC events				
ν	5400	∿130	23500	2300
$\bar{\nu}$	∿50	1120	∿240	2900

II. DILEPTON RESULTS

All four experiments have reported measurements of the fractional dilepton rate $\mu^-e^+/\mu^- = \sigma(\nu+Ne \to \mu^-+e^++...)/\sigma(\nu+Ne \to \mu^-+...)$ for neutrinos and/or the corresponding rate μ^+e^-/μ^+ for antineutrinos. The results, together with the techniques used and cuts employed, are summarized in Table II. All groups but FIIM identified the $e^\pm$ by requiring two independent visible signatures (e.g., spiralization to a point, bremstrahhlung) - FIIM instead used a fitting technique to determine energy loss inconsistent with a heavier particle. FIIM and BHS identified muons solely by the EMI, which requires that the muon candidate's momentum be greater than 4 GeV/c to reduce background and obtain reasonable geometric acceptance. WBHC required EMI confirmation when possible, but included events in which the muon candidate geometrically missed the EMI, but had the highest transverse momentum with respect to the neutrino direction (3 out of their 15 events falling in this category). CB was unable to use the EMI due to very high background in the EMI chambers. This group instead accepted the highest momentum noninteracting negative as a muon, then calculated the background by using the positive tracks, presumably all hadrons, to evaluate the interaction probability, then corrected the noninteracting negative sample using the observed interacting negatives to infer the number of leaving hadrons.

The most important backgrounds arise from (anti)neutrino CC events in which an asymmetric Dalitz decay or close pair fakes a single $e^\pm$ and from $(\bar{\nu})_e$ events in which a hadron simulates a muon. The former falls quickly with the $e^\pm$ momentum, and requires a momentum cut to reduce it to acceptable levels - 800 MeV/c for WBHC and BHS, and 300 MeV/c for CB.

The three measurements of μ^-e^+/μ^- are consistent, but only the BCS group obtained a clear antineutrino dilepton signal, the FIIM experiment determining an upper limit based on one questionable event. The results appear to be consistent with the charm model in which the $e^\pm$ is a product of the semileptonic decay of a charmed hadron, itself resulting from the fragmentation of a charmed quark created by the charged current from a d or s-quark by a neutrino, or an $\bar{s}$-quark by an antineutrino. In Fig. 1, the measurements,[7] corrected for the loss of events due to the $e^\pm$ momentum cut, are shown with a prediction of the model for the dilepton rate υ. neutrino energy. The most uncertain parts of this calculation are the form of the charm fragmentation function and the average charm semileptonic branching ratio, here taken to be 5%. It is interesting to note that the bubble chamber results are concentrated in the energy region where the model predicts a slow rise to the scaling region - the so-called slow-rescaling[8] method used in the computation. In contrast, counter experiments, which presumably study the same process, but with dimuon final states, can see only a small fraction of the total production of charm at these energies, measure of the 4 GeV minimum usually imposed on the muon momentum.

In the context of the charm model we expect significantly more strange particles than the ∿ 30% neutral strange particles per event inferred from νp interactions; if the charmed quark is produced equally from d and s-quarks, there should be in addition 1.5 strange particles, or about 0.75

TABLE II

Summary of delepton results.

	WBHC 3	FIIM 4	CB 5	BHS 6
Criteria				
$e^{\pm}$ ID	2 signatures	fit for E loss	2 signatures	2 signatures
p_e cut	800 MeV	200 MeV	300 MeV	800 MeV
$\mu^{\pm}$ ID	EMI or max $p_\perp$	EMI	fastest leaving negative	EMI
p_μ cut	2 GeV	4 GeV	-	4 GeV
E_{vis}	10 GeV	7.5 GeV	-	10 GeV
Neutrinos				
$\mu^- e^+$ events[a]	$\frac{15}{0.36 \pm 0.1}$	-	$\frac{81-(12 \pm 9.5)}{0.65 \pm 0.1}$	$\frac{6-(0.6 \pm 0.3)}{0.71 \pm 0.10}$
above with V^os	10	-	15	1
neutral strange particles per event	$1.84^{+0.67}_{-0.50}$	-	0.6 ± 0.2	-
μ^- events	5400 ± 200	-	23500 ± 600	2264 ± 165
$\frac{\mu^- e^+}{\mu^-}$ (%)	0.77 ± 0.3	-	0.5 ± 0.15[b]	$0.34^{+0.23}_{-0.13}$
Antineutrinos				
$\mu^+ e^-$ events[a]	-	$\frac{1-(0.2 \pm 0.2)}{0.7}$	-	$\frac{3-(1.1 \pm 0.4)}{0.69 \pm 0.10}$
above with V^os	-	0	-	1
μ^+ events	-	1120	-	2866 ± 211
$\frac{\mu^+ e^-}{\mu^+}$ (%)	-	< 0.5 (90% conf.)	-	$0.10^{+0.13}_{-0.07}$

(a) Background subtraction and efficiency corrections are explicitly shown.

(b) The values shown give (0.45 ± 0.10)% for this ratio; the quoted result has been rounded to one digit, and the error increased to cover additional systematics (M. Murtagh, private communication).

neutral strange particles per event. The total then, one neutral strange particle per event, lies between the CB result of 0.6 ± 0.2 and the WCBH measurement of $1.84^{+.63}_{-.53}$. However, the two measurements are statistically incompatible, the origin of which is not understood.

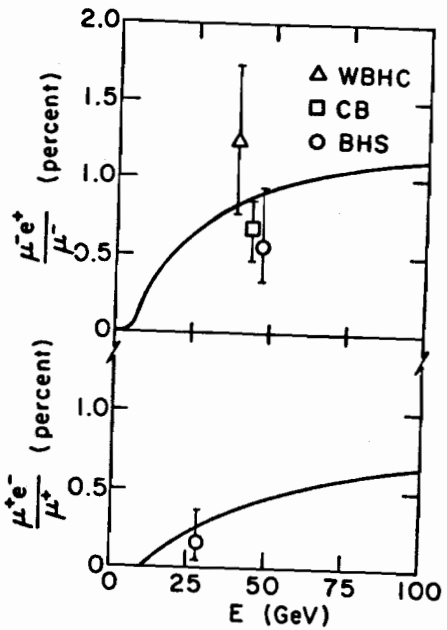

Fig. 1. Dilepton rates as a function of neutrino energy. The points are plotted for the approximate average energy of each experiment, and have been corrected for the loss of events due to the electron energy threshold using the calculation of Ref. 7. The curve represents the charm production ratio times an effective branching ratio of 15%.

III. ANTINEUTRINO SCALING VARIABLE DISTRIBUTIONS

FIIM has recently reported[9] on scaling variable distributions obtained from their $\bar{\nu}$ Ne data. Events were selected if the μ^+ candidate had a momentum greater than 4 GeV/c and was identified by the EMI and if the visible hadron energy exceeded 2 GeV. These cuts restrict the scaling variable y* to the range $2/E \leq y \leq 1 - 4E$, where E is the anti-neutrino energy in GeV, but do not affect the other scaling variable, x. The 611 events then were corrected for the EMI geometrical acceptance, a factor ranging from 0.6 to 0.96 depending on the muon angle and energy. Finally the missing neutral energy was accounted for in an average sense by increasing the observed hadron momentum for each event by 20% plus an additional 1.2 GeV.

Studying the y dependence, they fit the cross section with the form

$$\frac{d\sigma}{dy} \propto \frac{1+B}{2}(1-y)^2 + \frac{1-B}{2}$$

which assumes the Callan-Gross relationship.** In the quark model context, the first term represents the contribution of quarks, the second anti-quarks from the sea. Figure 2 shows the fit for all x and the lower energies. Combining all x and E, they find $B = 0.75^{+0.05}_{-0.06}$, corresponding to an anti-quark momentum fraction $\bar{Q}/(Q+\bar{Q}) = (14 \pm 3)\%$. (This quantity is 8% for the quark distributions of Field and Feynman.) The energy dependence of B, Fig. 5d, is consistent with no change, and the recent CERN counter experiment.[10]

Examining the x dependence, Fig. 3, we see further confirmation of the quark picture. The model predicts that the effect of antiquarks is enhanced by a factor of 3 relative to quarks, in comparison with deep inelastic electroproduction data. Figure 3 shows the data and normalized to it, the Feynman and Field distribution assuming no charm production. For comparison, the effect of charm production, and the distributions for νN and eN scattering are also shown, all normalized to the same quark contribution. Since the antiquark sea is confined to small x, the shape of dσ/dx for $\bar{\nu}$N should show an enhancement at low x with respect to electoproduction. As can be seen, the data clearly show this effect.

The concentration of the effect of antiquarks at small values of x also shows up in the x-dependence of B. The fraction of momentum carried by

---

* The scaling variables are defined by $y = E_h/E$, where E_h is the hadron energy, and $x = Q^2/2ME_h$, with Q^2 the momentum transfer to the nucleon, and M the nucleon mass.

** An additional term proportional to y^2 is required if the Callan-Gross relationship is not satisfied, which is in fact expected to be the case in the threshold region for production of a heavy quark, such as charm.

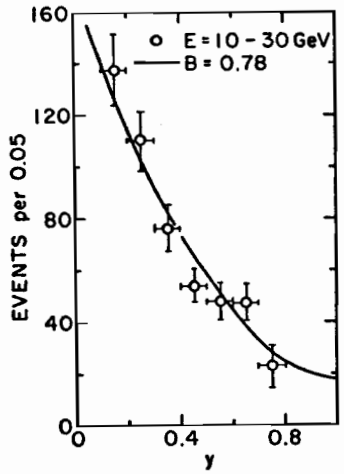

Fig. 2. The FIIM antineutrino y distribution for E=10-30 Gev, compared with the fit B parameter.

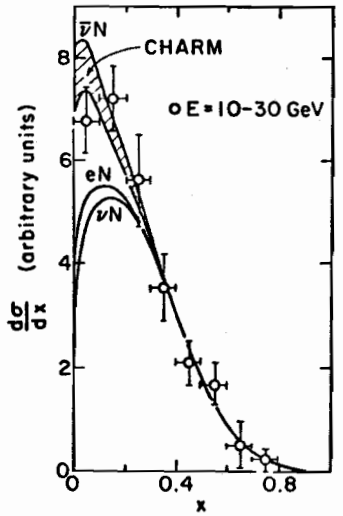

Fig. 3. The FIIM antineutrino x compared with the FF prediction. The crosshatched area represents the effect of charm production. For comparison, the predictions for eN and νN scattering are also shown, all normalized to the same quark contribution.

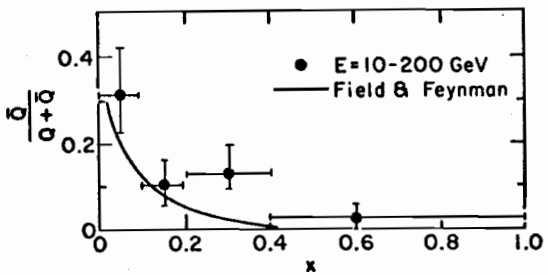

Fig. 4. The FIIM fits to B, expressed as the antiquark momentum fraction, for the ranges of x shown, and the Field and Feynman prediction.

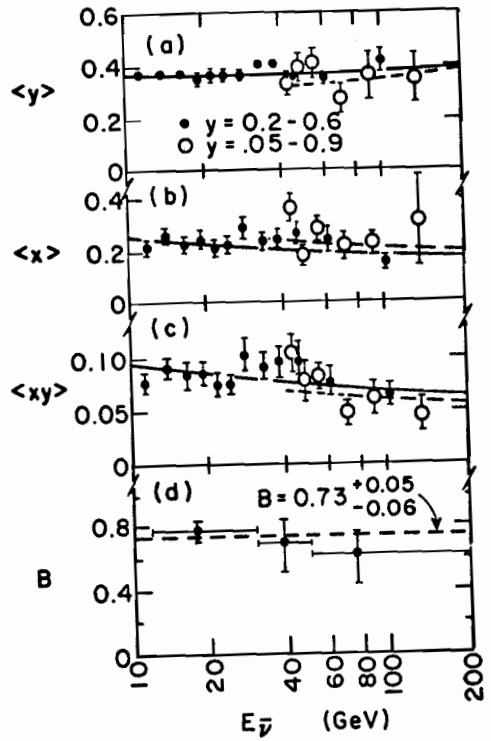

Fig. 5. (a)-(c): The average values of y, x, and xy, respectively, as a function of antineutrino energy, compared with the form $\langle x \rangle = E^{-0.14}$ for y in the range 0.2 to 0.6 (solid data points and solid line) and for y in the range 0.05 to 0.9 (open points and broken line). (d): The values of the B parameter obtained for the three energy ranges shown.

antiquarks, (1-B)/2, is shown on Fig. 4 along with FF prediction. The expected decrease with x is apparent, although not as rapid as the prediction.

Turning to the energy depedence of $\langle x \rangle$, Fig. 5b, a scale breaking effect similar to that seen in electron and muon deep inelastic scattering is perhaps seen. Parametrizing this by $\langle x \rangle \propto E^{-b}$, they find $b = 0.14 \pm 0.06$, to be compared with $b = 0.15$ determined from the electron and muon data. If the x and y dependence factorize, and $\langle y \rangle$ is independent of energy, as is the case in Fig. 5a, then $\langle xy \rangle$, Fig. 5c, should show the same variation as $\langle x \rangle$; in fact there is a significant break around 40 GeV instead of the gentle decline which is expected.

IV. PROTON - NEUTRON SEPARATION

The FIIM group has reported preliminary[11] results using a technique to measure the ratio of $\bar{\nu}n$ to $\bar{\nu}p$ charged current cross sections, based on total observed charge. Using the charged current data described in the previous section, they eliminate any event with a track of uncertain charge, and, not counting proton stubs, determine the net charge distribution for the remaining 670 events, shown in Fig. 6. Since the initial charge of the $\bar{\nu}n$ and $\bar{\nu}p$ states is respectively 0 and +1, the tail toward positive charge suggests that the effect of reinteraction is to increase the charge, and the nearly constant ratios of adjacent charge states, +3 to +2, +4 to +3, etc. suggests that the probability for the charge to increase by n units is simply $(W_+)^n$, where W_+ is the probability to increase by one unit. Then the probability of no change is $W_o = 1 - \sum_{n=1}^{10} W_+^n$. If one makes this assumption, only one parameter remains, the cross section ratio $\eta = \sigma(\bar{\nu}n)/\sigma(\bar{\nu}p)$. A fit to the data gives $W_+ = 0.35$, $W_o = 0.46$, and $\eta = 0.59 \pm 0.07$, the latter consistent with the quark model prediction 0.55. The presence of $\sim 1\%$ of the events with net negative charge indicates an uncertainty in determining the net charge, partly due to uncertainty in ascribing slow protons solely to nuclear breakup. An uncertainty in η of 0.05 has been included to allow for this.

Having determined W_+, η can then be determined as a function of the scaling variables x and y. The picture of the reinteraction being independent of the initial interaction is checked by examining the quantities ΣP_x, W, and Q^2 vs. the mean and first moment of the net charge distribution - no effect is seen. The results, shown in Fig. 7, are consistent with the expectation from the Field and Feynman distribution, especially the dramatic fall as x varies from 0 to 1.

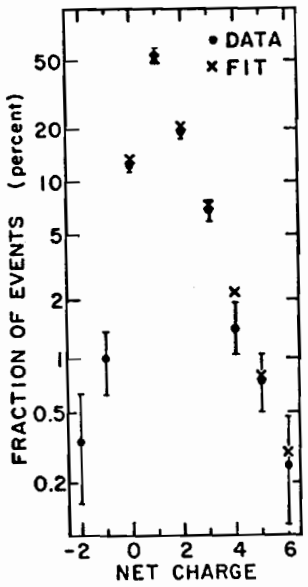

Fig. 6. The net charge distribution of the FIIM data, excluding stubs, compared with the fit described in the text. The fit predicts no events with negative charge.

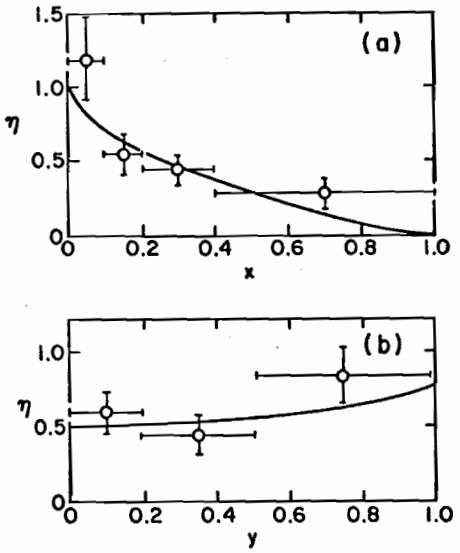

Fig. 7. The neutron to proton cross section ratio, η, as a function of x in (a) and y in (b) compared with the Field and Feynman prediction.

V. HADRON PHYSICS WITH $\overset{(-)}{\nu}_e$'s

The BHS collaboration, having obtained a carefully-studied set of 74 ν_e and 47 $\bar{\nu}_e$ events as a result of their dilepton search, has studied the hadron states in these events.[12] The y distributions, Fig. 8, are consistent with the muon neutrino equivalents, that is, approximately flat for ν and decreasing for $\bar{\nu}$. This represents a check of μ-e universality and the electron neutrino interpretation of these events.

Then they obtain the inclusive laboratory rapidity for all charged hadrons, defined with respect to the total visible hadronic momentum. This is shown separately for ν_e and $\bar{\nu}_e$ on Fig. 9, normalized to the total cross section so that the area under the curves represents the average charged hadron multiplicity. The effect of the nucleus on the hadronic state can then be studied by comparison with hydrogen data, which is facilitated because the distributions in hadronic energy, or w, are similar. The comparisons, ν_eNe with ν_μp and $\bar{\nu}_e$Ne with $\bar{\nu}_\mu$p, in fact show a significant increase for neon with respect to hydrogen in the region of small rapidities, that is, the target fragmentation region. The ratio of the two curves in the region from -1 to +1, representing the factor by which multiplicity increases in this region, is 2.2 ± 0.3 for neutrinos and 2.1 ± 0.4 for antineutrinos. A similar factor has been observed in purely hadronic interactions.

When comparison is made of the combined ν_e and $\bar{\nu}_e$ rapidity distributions with πNe data at approximately the same hadron invariant energy, Fig. 10, no such difference is seen in the small rapidity region. The conclusion, which is reinforced by the study of transverse momentum, multiplicity, and the momentum distribution of identified protons, is that the effect of the nucleus apparent in the comparison of νNe with νp interactions is the same as that observed with hadron beams.

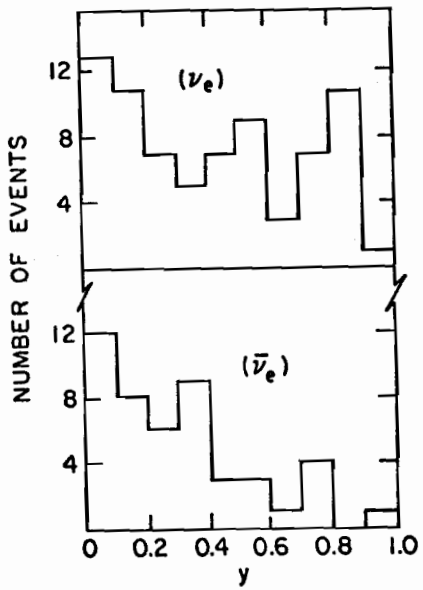

Fig. 8. y distribution for ν_e and $\bar{\nu}_e$ events from the BHS data.

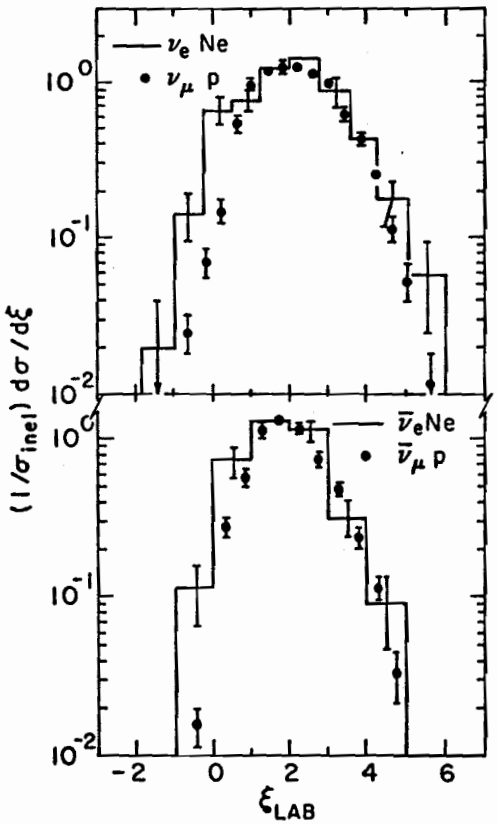

Fig. 9. Comparison of laboratory rapidity, ξ, for $\nu_e(\bar{\nu}_e)$ Ne and $\nu_\mu(\bar{\nu}_\mu)$ p interactions.

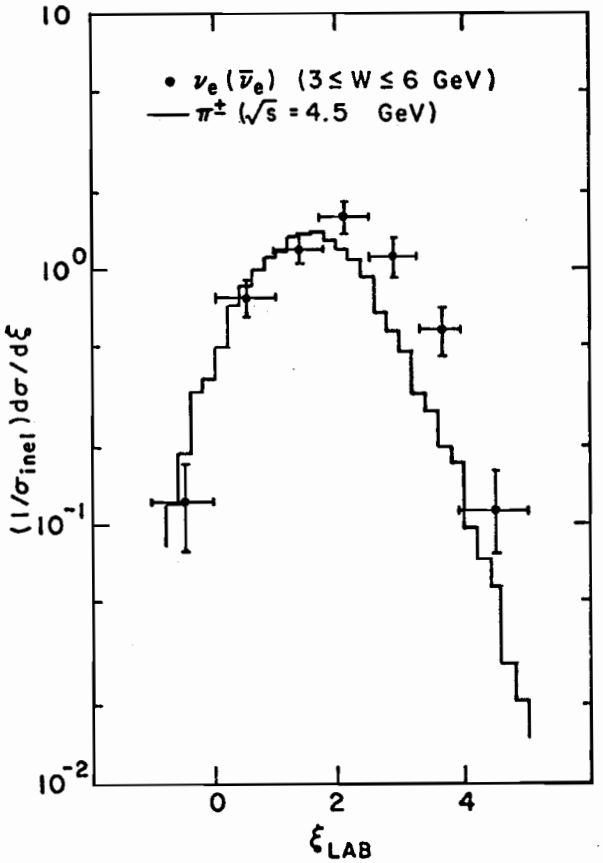

Fig. 10. Comparison of laboratory rapidity for $\nu_e(\bar{\nu}_e)$Ne (combined) and πNe.

REFERENCES

(1) R. D. Field and R. P. Feynman, Phys. Rev. 15 (1977) 2590.

(2) M. Holder et al., Phys. Lett. 69B (1977) 377.

(3) J. von Krogh et al., Phys. Rev. Lett. 36 (1976) 710; P. Bosetti et al., Phys. Rev. Lett. 38 (1977) 1248.

(4) J. P. Berge et al., Phys. Rev. Lett. 38 (1977) 266.

(5) C. Baltay et al., Phys. Rev. Lett. 39 (1977) 62.

(6) H. C. Ballagh et al., Phys. Rev. Lett. - to be published.

(7) V. Barger, T. Gottschalk, and R. J. N. Phillips, Multihadron Semi-leptonic Decays of Charmed Mesons, University of Wisconsin preprint CCO-564 (1977).

(8) R. Michael Barnett, Phys. Rev. Lett. 36 (1976) 1163.

(9) Fermilab-IHEP-ITEP-Michigan Neutrino Group, Phys. Rev. Lett. 39 (1977) 382.

(10) M. Holder et al., Phys. Rev. Lett. 39 (1977) 433.

(11) V. I. Efremenko et al., submitted to ν77 Conference, Elbrus, USSR.

(12) T. H. Burnett et al., submitted to ν77 Conference, Elbrus, USSR, and University of Washington preprint VTL-PUB-44.